Supplementary Information for:

Stress Changes the Material State of a Bacterial Biomolecular Condensate and Shifts its Function from mRNA Decay to Storage

Luis A. Ortiz-Rodríguez[1], Hadi Yassine[2,3], Ali Hatami[4], Vidhyadhar Nandana[2], Christopher A. Azaldegui[5], Jiayu Cheng[1], Yingxi Zhu[4], Jared M. Schrader[2,3*], Julie S. Biteen[1,5*]

[1]Department of Chemistry, University of Michigan, Ann Arbor, MI 48109 USA.

[2]Departments of Chemistry and Biological Sciences, Wayne State University, Detroit, MI 48202 USA.

[3]Department of Biology, Indiana University, Bloomington, IN 47405 USA.

[4]Department of Chemical Engineering and Materials Science, Wayne State University, Detroit, MI 48202 USA.

[5]Doctoral Program in Chemical Biology, University of Michigan, Ann Arbor, MI 48109, USA.

[*] To whom correspondence should be addressed: jsbiteen@umich.edu, jaschrad@iu.edu

Contents:

Supplementary Figures

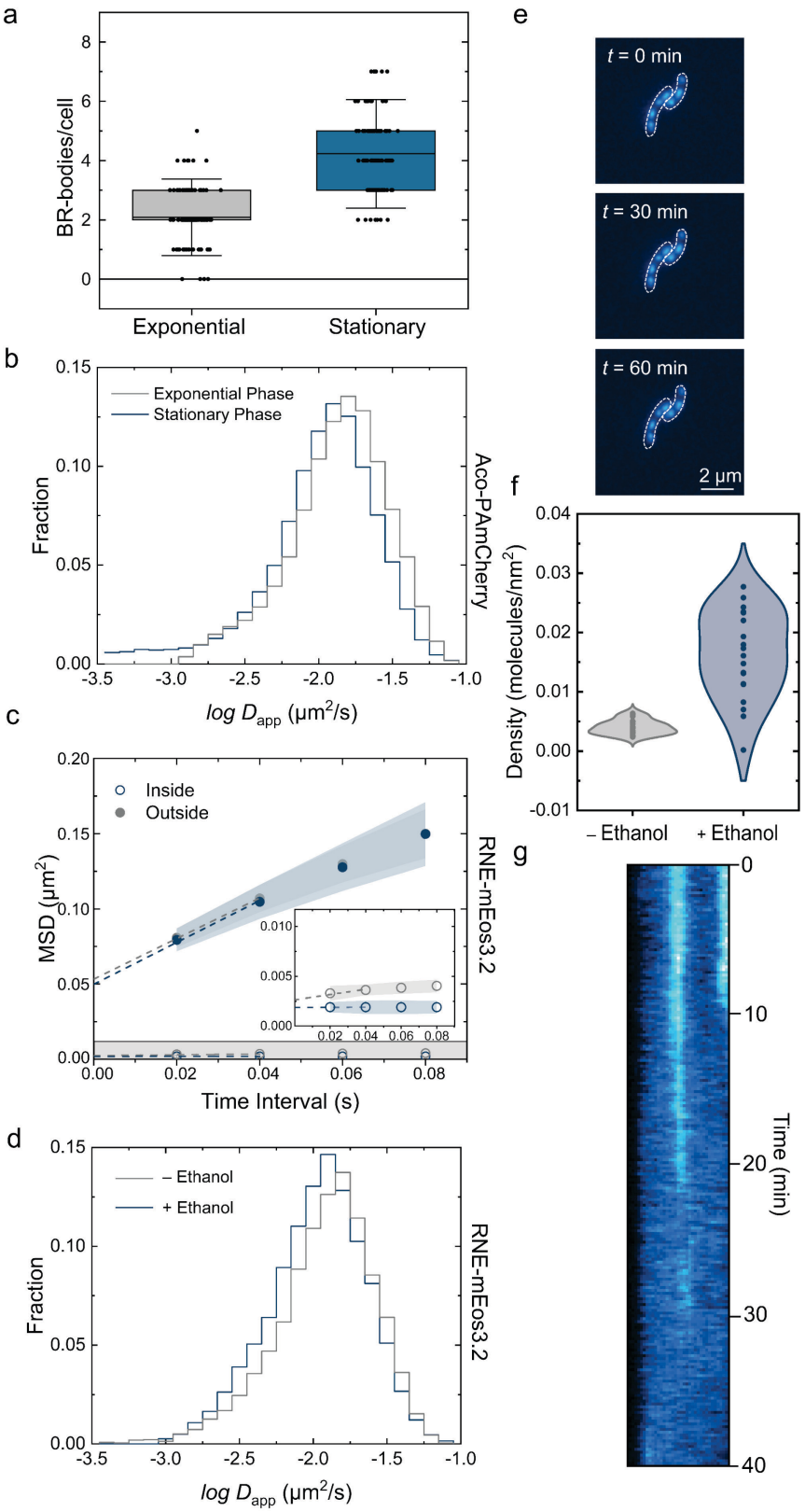

Supplementary Figure 1 | Phase-dependent and chemically induced changes in BR-body dynamics, composition, and material state.

Supplementary Figure 1 | Phase-dependent and chemically induced changes in BR-body dynamics, composition, and material state. (a) Number of BR-bodies per cell in exponential and stationary phase. Error bars indicate the standard deviation. Sample sizes were n = 131 cells for exponential phase and n = 109 cells for stationary phase. Horizontal lines within the boxes indicate the mean, and box boundaries mark the 25th and 75th percentiles. (b) Distributions of diffusion coefficients of aconitase-PAmCherry trajectories inside BR-bodies during exponential and stationary phase. (c) Mean squared displacement (MSD) as a function of time lag for RNE-mEos3.2 trajectories inside and outside BR-bodies in exponential and stationary phases. These curves were used to extract ensemble-averaged diffusion coefficients. Inset: Enlarged view of the highlighted gray region, showing the MSD as a function of time interval for RNE-mEos3.2 trajectories within BR-bodies. Shaded regions indicate the SEM. (d) Diffusion coefficient distributions of RNE-mEos3.2 trajectories inside BR-bodies during exponential phase, with or without treatment with 10% ethanol. (e) Representative images of *C. crescentus* cells (white outlines) expressing RNE-mEos3.2 (blue) over time, *t*, during exponential phase with treatment with 10% ethanol. Scale bar: 2 μm. Similar results were obtained from three independent colony replicates. (f) Molecular density of RNE-mEos3.2 inside BR-bodies in exponential phase with and without 10% ethanol treatment. $N = 20$ clusters. (g) Representative kymograph of a stationary phase cell (x-axis) expressing RNE-mEos3.2 following treatment with 5% 1,6-hexanediol, showing dissolution of BR-bodies over the course of 40 min.

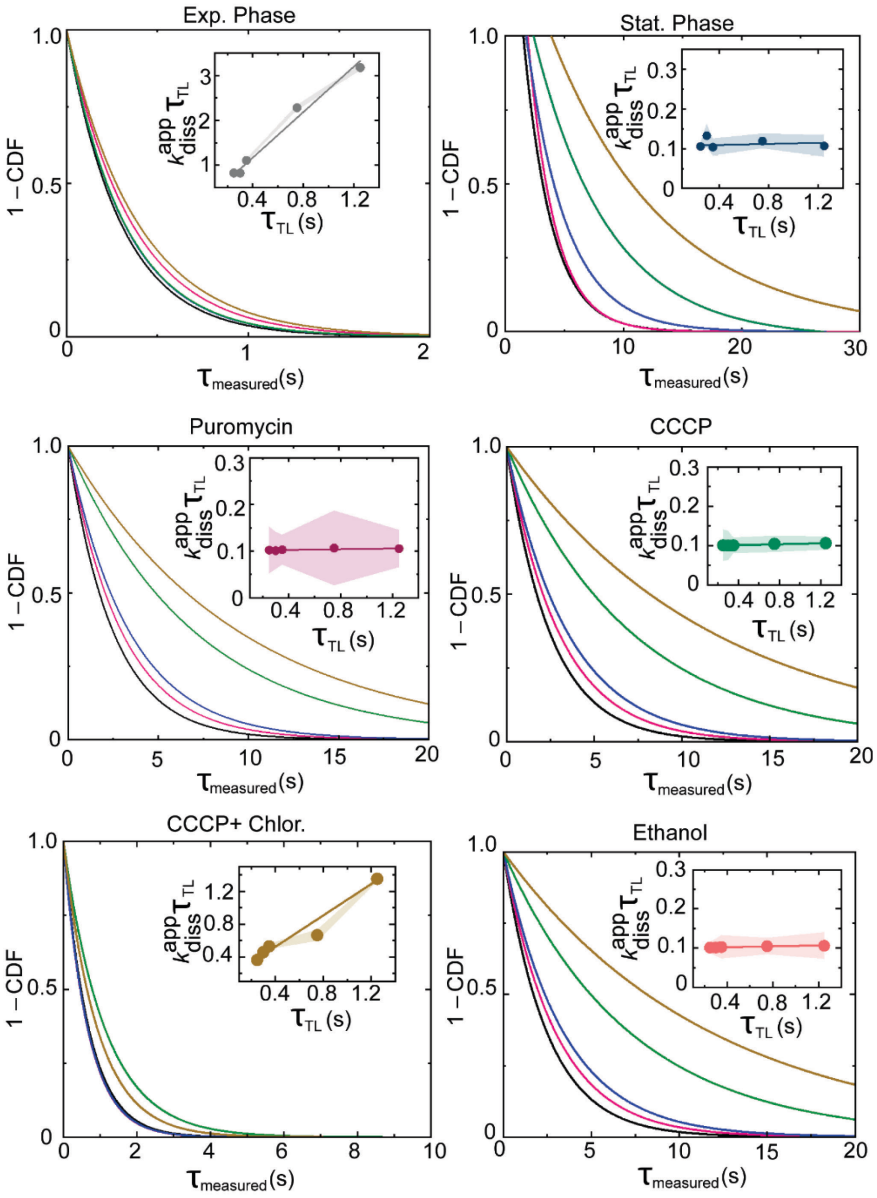

Supplementary Figure 2 | Change in RNE-mEos3.2 residence time inside BR-bodies in *C. crescentus* cells across growth phases and under different acute stress conditions. Fitted exponential decay curves from plots of 1 minus the cumulative probability function (CDF) of observed residence times imaged by slow tracking ($t_{integration}$ = 250 ms) using continuous imaging (black) and time delays (pink, blue, green, and gold for 300, 350, 750, and 1250 ms, respectively). The inset within each (1 – CDF) vs. $\tau_{measured}$ plot shows the linear fit of $k_{diss}^{app}\tau_{TL}$ *vs.* τ_{TL}, from which the dissociation rate constant, $k_{diss}^{app}\tau_{TL}$, which is the reciprocal of the residence time, is extracted (Methods Equation 1). For each $\tau_{measured}$, at least three biological replicates were analyzed.

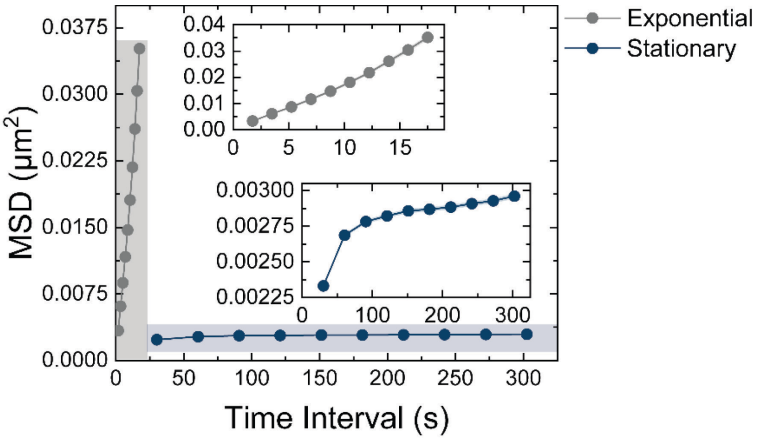

Supplementary Figure 3 | Mean squared displacement (MSD) as a function of time interval for BR-bodies during exponential and stationary phase. BR-bodies in stationary phase cells are nearly immobile compared to those in exponential phase cells, reflecting a substantial decrease in mobility. Due to the large difference in diffusion, both curves are also shown in insets (highlighted by colored rectangles) to aid visualization on appropriate scales. Number of trajectories analyzed: 3,761 (exponential phase) and 12,265 (stationary phase).

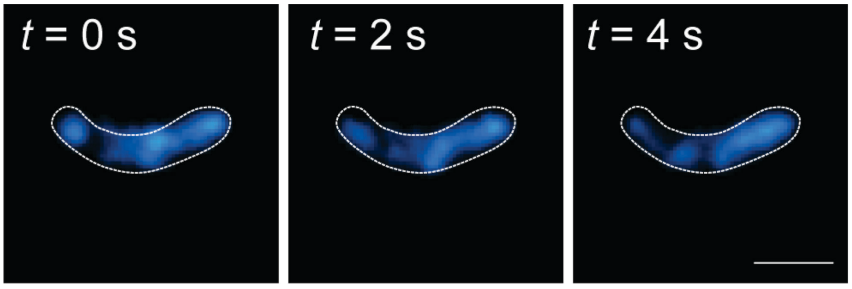

Supplementary Figure 4 | Representative images of *C. crescentus* cells (white outlines) and RNE-mEos3.2 (blue) following chloramphenicol (200 μg/mL) treatment as a function of imaging time. Scale bar: 500 nm. Similar results were obtained from three independent colony replicates.

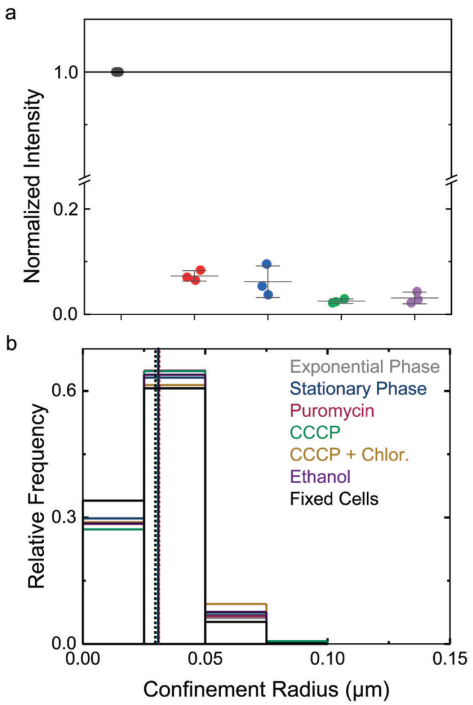

Supplementary Figure 5 | Comparison of translation levels and diffusivity of BR-bodies in *C. crescentus* cells across growth phases and following acute treatments. (a) Relative translational levels in exponential phase in the presence and absence of CCCP, both CCCP and chloramphenicol, ethanol, and puromycin using Biorthogonal Non-Canonical Amino Acid Tagging (BONCAT). Error bars: standard deviation from three replicates (dots). Mean shown as the center line. (b) The distributions of confinement radii for RNE-mEos3.2 focus trajectories in living cells (colors) were compared to the confinement radii of trajectories in fixed cells (black) to differentiate between diffusing and static foci. Only the first eight frames of each focus trajectory were used for this analysis. Vertical dashed lines: medians of the distributions.

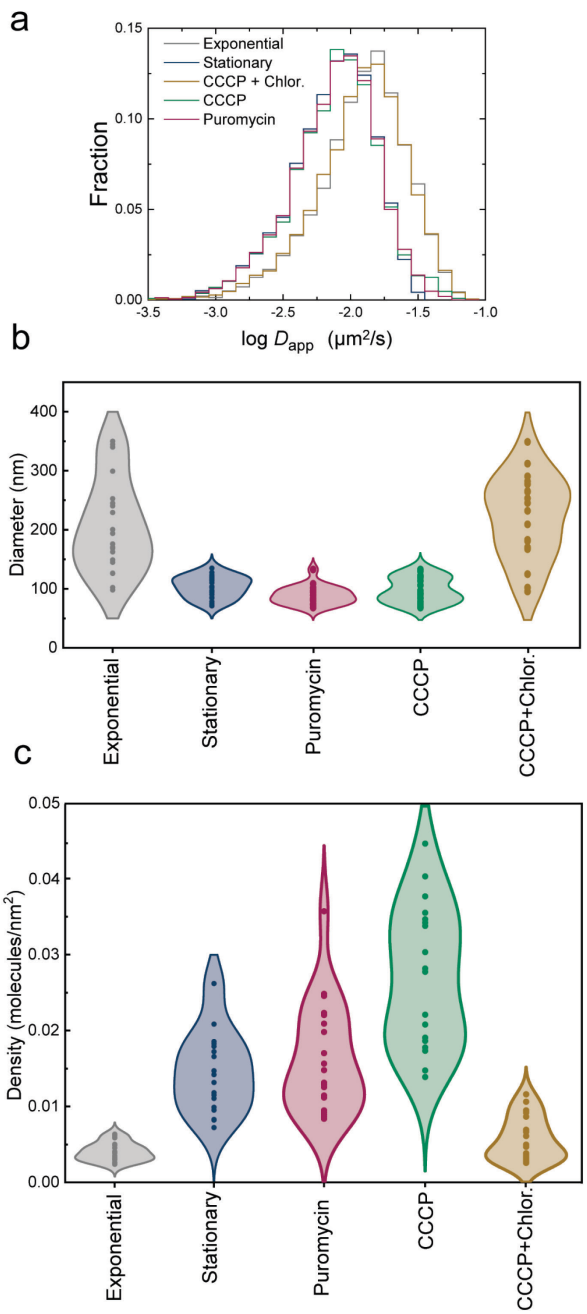

Supplementary Figure 6 | Comparison of (a) apparent diffusion coefficient distributions, (b) BR-body diameters, and (c) BR-body molecular density across growth phases and acute stress conditions. Number of trajectories analyzed in (a): 5,001 (exponential phase), 6,347 (stationary phase), 2,126 (puromycin), 1,637 (CCCP), and 1,441 (CCCP + chloramphenicol). Number of clusters analyzed in (b) and (c): 20.

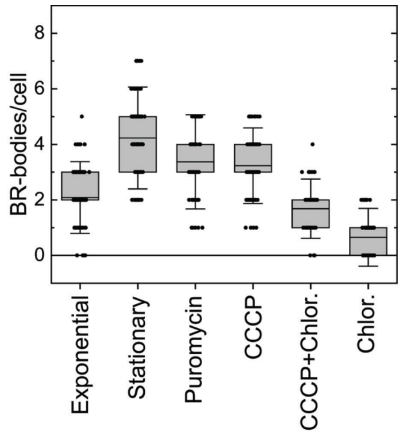

Supplementary Figure 7 | Quantification of the number of BR-bodies per cell as a function of growth phase or acute stress. Error bars indicate the standard deviation. We report the mean ± SD and 95% confidence intervals (CIs) for each condition. For exponential phase, the mean difference relative to stationary phase: –2.14 (95% CI: –2.41 to –1.86), to puromycin: –1.28 (95% CI: –1.57 to –0.98), to CCCP –1.18 (95% CI: –1.40 to –0.95), to CCCP+chloramphenicol: +0.37 (95% CI: 0.16 to 0.57), and to chloramphenicol: +1.42 (95% CI: 1.20 to 1.64). For stationary phase, the mean difference relative to puromycin: +0.86 (95% CI: 0.52 to 1.20), to CCCP: +0.96 (95% CI: 0.68 to 1.25), to CCCP+chloramphenicol: +2.50 (95% CI: 2.23 to 2.77), and to chloramphenicol: +3.55 (95% CI: 3.27 to 3.83). Horizontal lines within the boxes indicate the mean, and box boundaries mark the 25th and 75th percentiles.

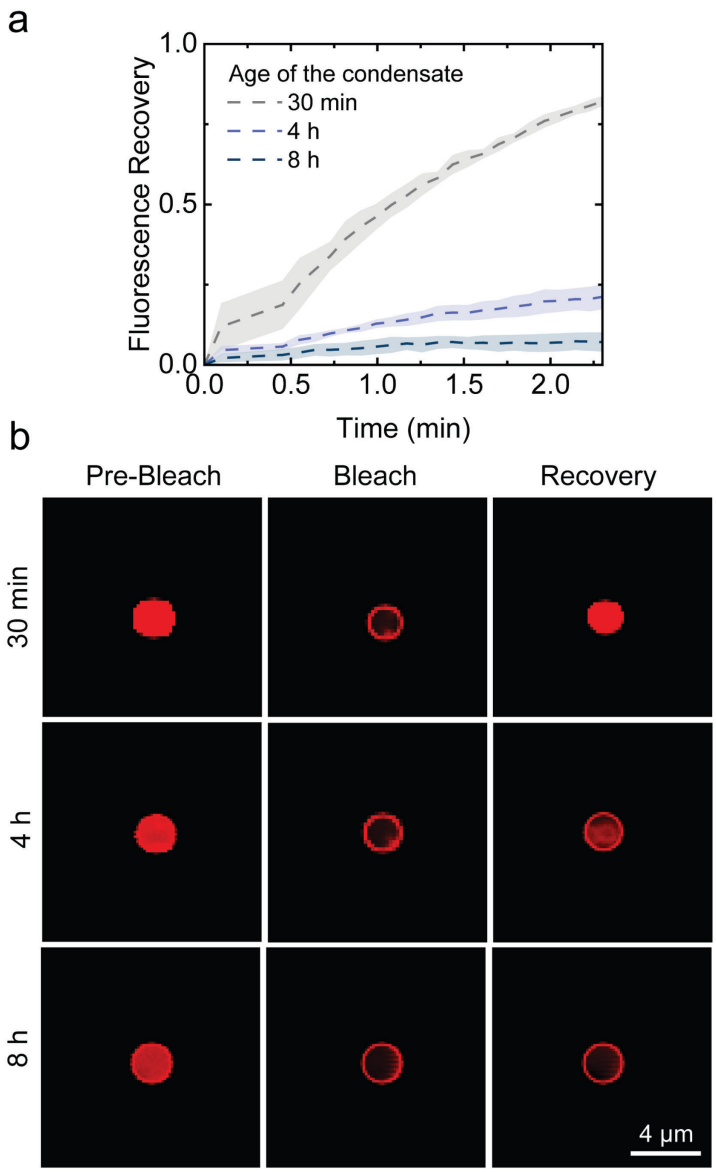

Supplementary Figure 8 | Aging of *in vitro*-reconstituted RNE condensates leads to decreased internal dynamics as measured by FRAP. (a) Fluorescence recovery after photobleaching (FRAP) and (b) representative images of reconstituted RNE-Cy5 *in vitro* condensates at the indicated time points after formation. Error bars indicate the standard deviation. Three replicates were obtained for each condition.

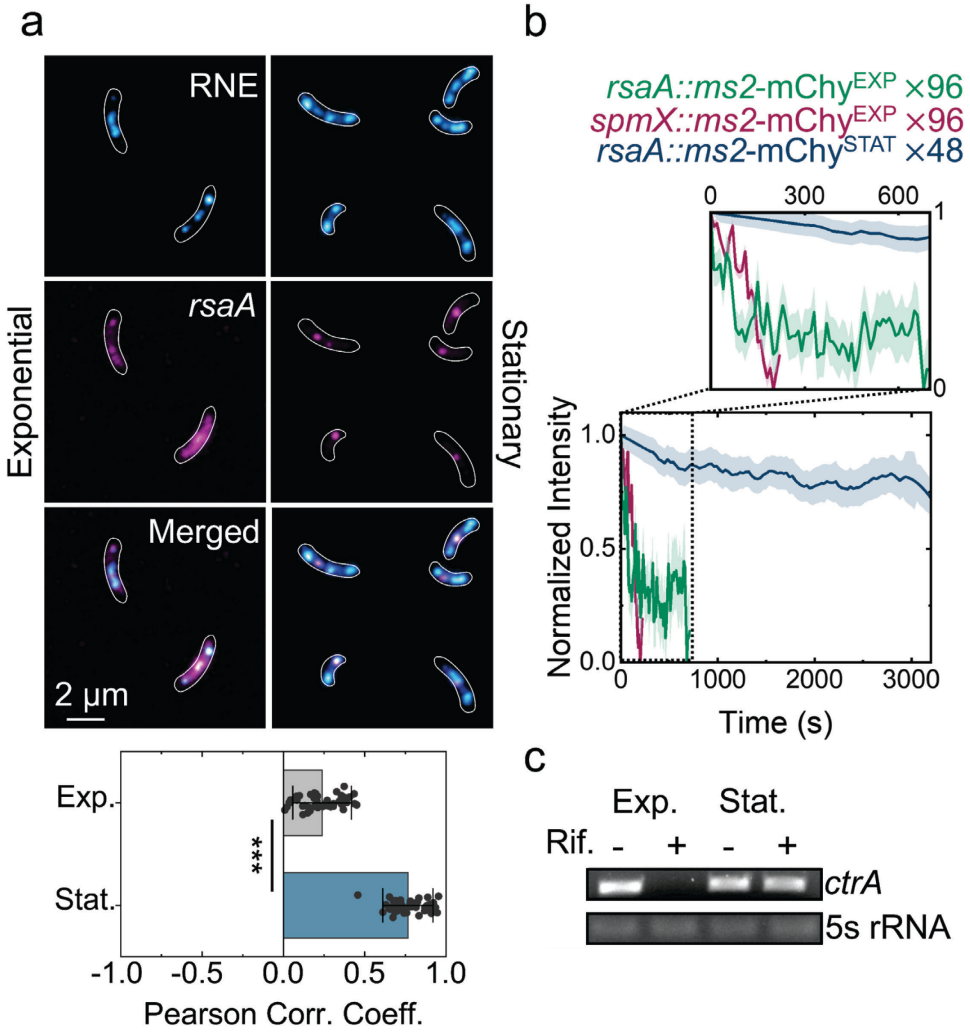

Supplementary Figure 9 | Comparison of mRNA transcript stability between exponential and stationary phases. (a) Representative two-color images showing higher recruitment of the *rsaA* (48× array) transcript (magenta) to BR-bodies (blue) in *C. crescentus* cells (white outlines) during stationary phase (left) relative to exponential phase (right). Bottom: Differences in recruitment quantified by the Pearson correlation coefficients between channels. Error bars: standard deviation from 50 cells analyzed per phase. Two-tailed Welch's test: $p = 1.18 \times 10^{-40}$. Circles indicate the PCC of each cell. Similar results were obtained from three independent colony replicates. (b) Fluorescence decay profiles of *rsaA* and *spmX* foci. The line indicates the mean, and the shaded region indicates the standard deviation. (c) Full-length *ctrA* mRNA remains stable in stationary phase. Total RNA was collected from cells in exponential phase and stationary phase with or without a 16-minute rifampicin treatment. The mRNAs were reverse transcribed into full-length *ctrA* or 5S rRNA cDNA, which was then used as a template to amplify the PCR product. 5S rRNA was used as a loading control. The 5S rRNA was PCR amplified for 10 cycles, while *ctrA* was amplified for 25 – 30 cycles.

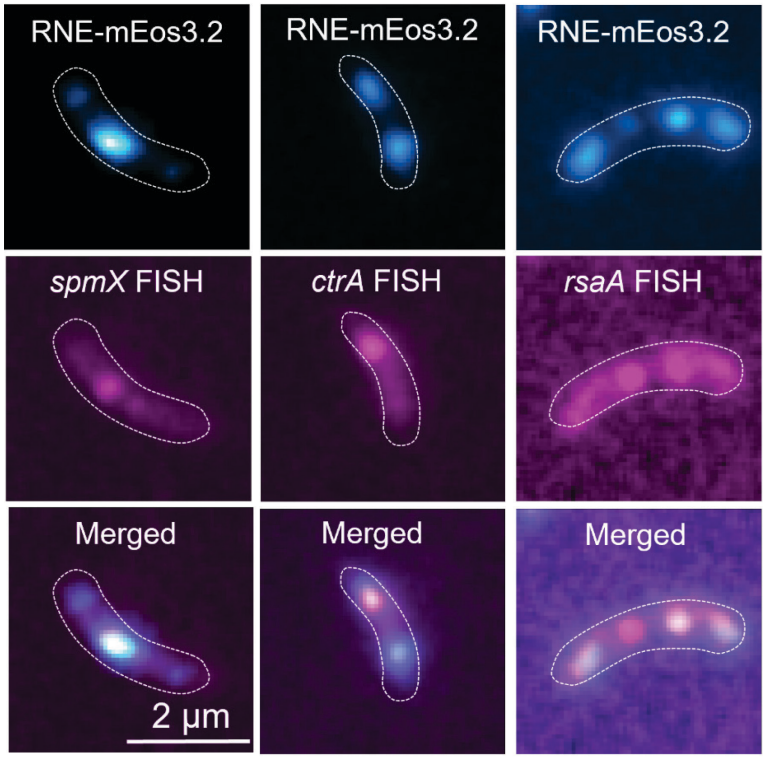

Supplementary Figure 10 | mRNA fluorescence in situ hybridization (FISH) of selected transcripts during stationary phase. Cyan: Fluorescence images of RNE-mEos3.2 in representative *C. crescentus* cells (white outlines). Magenta: mRNA FISH images of *spmX*, *ctrA*, and *rsaA* transcripts in the same *C. crescentus* cells, respectively. Similar results were obtained from three independent colony replicates.

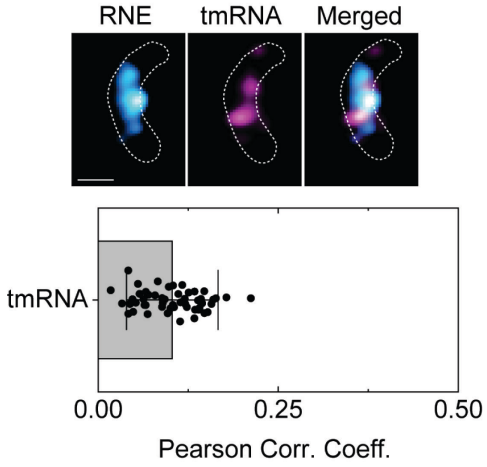

Supplementary Figure 11 | *ssrA*/tmRNA FISH (top) and quantification of colocalization profile using the Pearson correlation coefficient (bottom). Cyan: Fluorescence images of RNE-mEos3.2 in a representative *C. crescentus* cell (white outlines). Magenta: tmRNA FISH images. Scale bar: 500 nm. Error bars indicate the standard deviation of the Pearson correlation coefficients obtained for each of 50 cells. Similar results were obtained from three independent colony replicates.

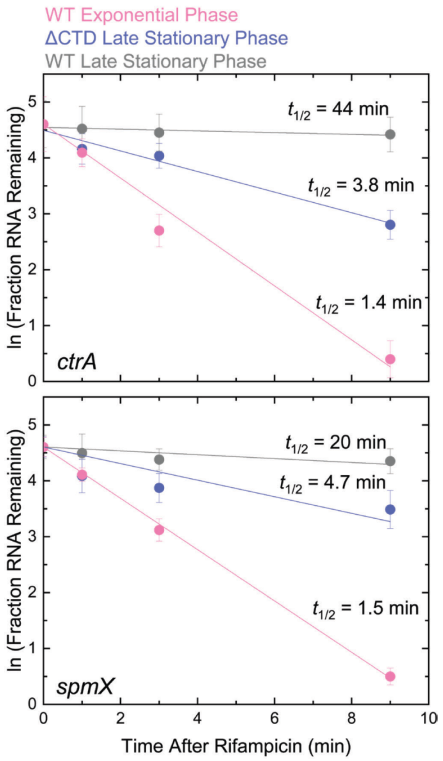

Supplementary Figure 12 | BR-body formation is required for robust mRNA stabilization during stationary phase. Fraction of RNA remaining over time as measured by mRNA FISH for *ctrA* and *spmX* transcripts in wild-type exponential phase (pink), wild-type late stationary phase (gray), and RNE-ΔCTD late stationary phase (blue). Transcripts are rapidly degraded in exponential phase and in the absence of BR-bodies (RNE-ΔCTD) but are significantly stabilized in wild-type stationary phase, indicating that BR-body formation is necessary for transcript protection during stress. Error bars: standard deviation from three biological replicates.

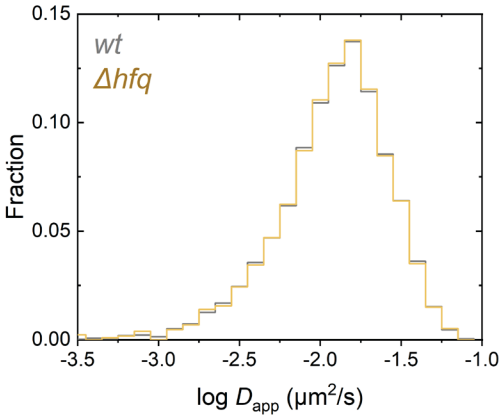

Supplementary Figure 13 | Apparent diffusion coefficient distributions of RNE-mEos3.2 within BR-bodies in wild-type and Δ*hfq C. crescentus* cells during exponential phase. The similarity in diffusion profiles indicates that the absence of Hfq does not affect RNE-mEos3.2 mobility within BR-bodies under these conditions. 2,441 and 5,001 trajectories were analyzed for Δ*hfq* and *wt*, respectively.

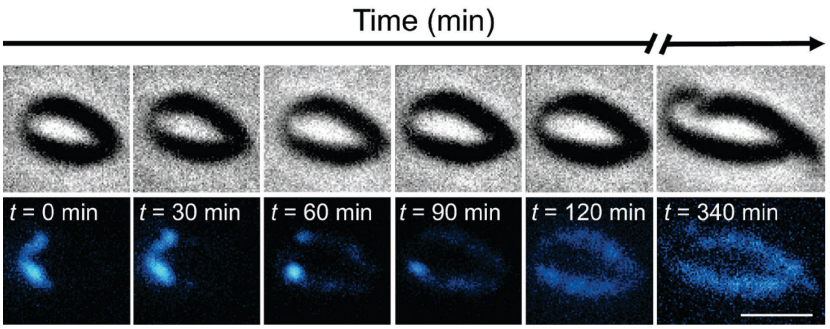

Supplementary Figure 14 | BR-bodies disassemble upon nutrient replenishment. Representative images of *C. crescentus* cells (top: phase contrast) and RNE-YFP (bottom: blue) as a function of imaging time, *t*. Fresh M2G medium was added at *t* = 0 min. Scale bar: 2 μm. Similar results were obtained from three independent colony replicates.

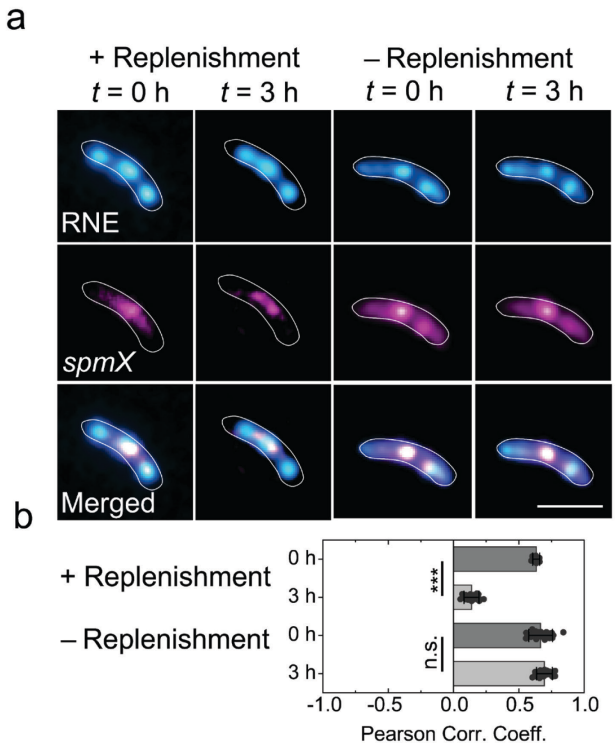

Supplementary Figure 15 | Recruitment of mRNA into the BR-bodies after nutrient replenishment mimics mRNA recruitment in exponential phase. (a) Representative two-color images showing the recruitment profile of the *spmX* transcript (magenta) to BR-bodies (blue) in *C. crescentus* cells (white outlines) at time, *t*, following nutrient replenishment (left) and without nutrient replenishment (right). Right: Control. Scale bar: 2 μm. Similar results were obtained from three independent colony replicates. (b) Differences in recruitment were quantified by the Pearson correlation coefficients between channels. Error bars: standard deviation from 50 cells analyzed per phase. Two-tailed Welch's *t*-test: $p = 7.05 \times 10^{-9}$ (+replenishment 0 h vs. + replenishment 3h) and 0.155 (–replenishment 0 h vs. –replenishment 3h). *** denotes $p < 0.001$. n.s. denotes $p > 0.05$.

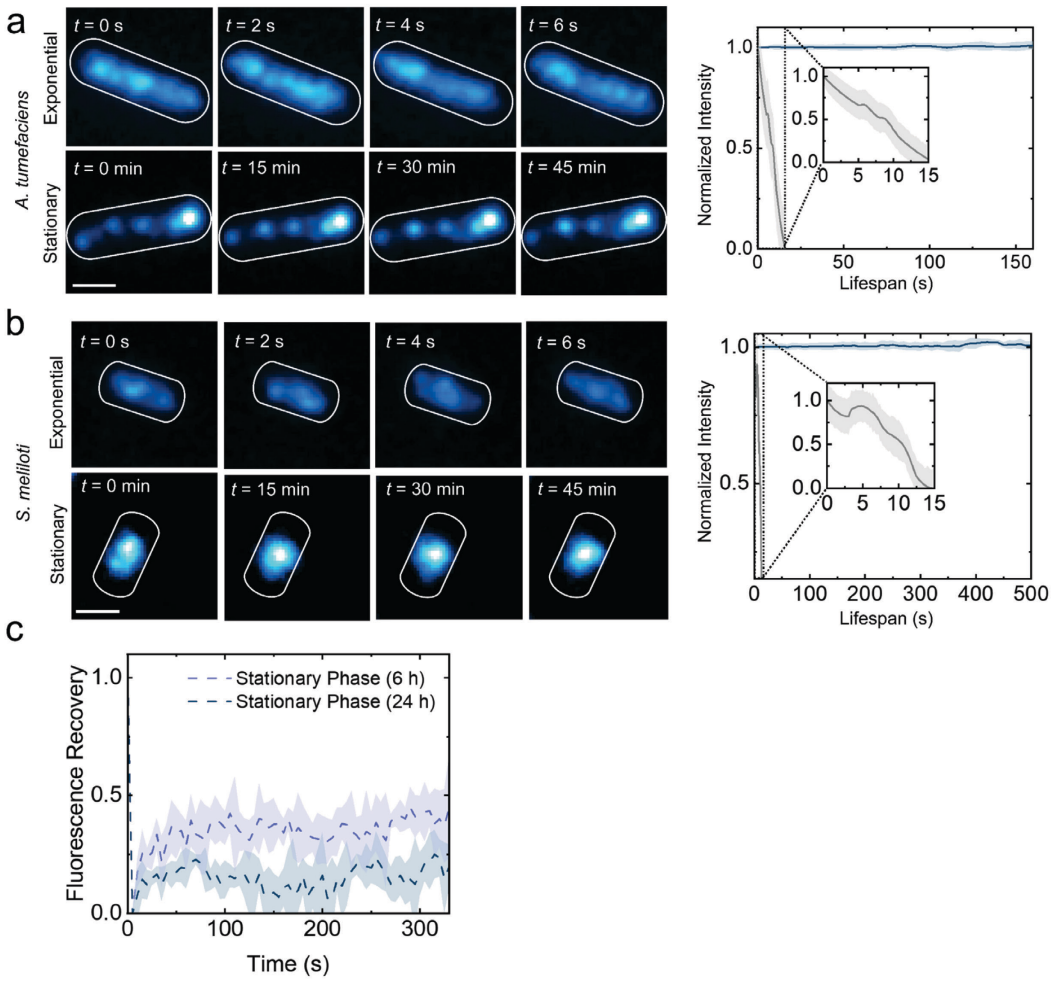

Supplementary Figure 16 | RNE dynamics in *Agrobacterium tumefaciens* and *Sinorhizobium meliloti* during exponential and stationary growth phases. (a) Lifespans of condensates in exponential and stationary growth phases of *A. tumefaciens*. Left: Representative images of RNE-YFP (blue) inside *A. tumefaciens* cells (white outlines) in each growth phase as a function of imaging time, *t*. Right: decay profiles of photobleaching-corrected focus intensities. Analyses include $N = 53$ foci (exponential) and $N = 65$ foci (stationary). The line indicates the mean, and the shaded region indicates the standard deviation. Similar results were obtained from three independent colony replicates. (b) Lifespans of condensates in exponential and stationary growth phases of *S. meliloti*. Left: Representative images of RNE-YFP (blue) inside *S. meliloti* cells (white outlines) in each growth phase as a function of imaging time, *t*. Right: decay profiles of photobleaching-corrected focus intensities. Analyses include $N = 26$ foci (exponential) and $N = 31$ foci (stationary). The line indicates the mean, and the shaded region indicates the standard deviation. Similar results were obtained from three independent colony replicates. (c) Fluorescence recovery after photobleaching (FRAP) of RNE-YFP in *A. tumefaciens* cells at early (6 h) and late (24 h) stationary phase. Dashed lines indicate the mean, and the shaded region indicates the standard deviation. Scale bars in (a) and (b): 1 μm.

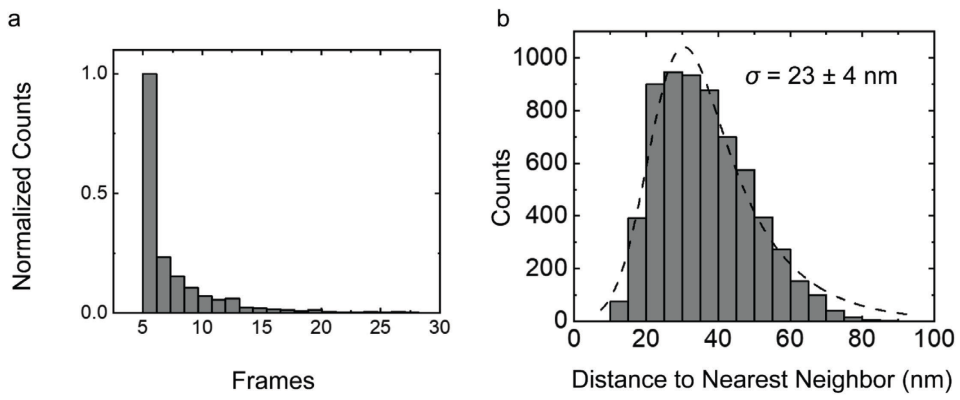

Supplementary Figure 17│Calculation of single-molecule RNE-mEos3.2 trajectory lengths and localization precisions in *C. crescentus cells*. *C. crescentus* cells expressing RNE-mEos3.2 were fixed, and single RNE-mEos3.2 molecules were photoconverted and then localized to obtain trajectories. (a) Distribution of trajectory lengths of RNE-mEos3.2 in fixed cells (imaging frame time: 20 ms). Trajectories lasting fewer than 4 frames were not used in our analysis. (b) Distribution of the nearest neighbor distances, d, in fixed cells based on repeated localizations of the same RNE-mEos3.2 molecule. The nearest neighbor distribution histogram, $p(d)$, was fit (dashed line) to Equation (2), as described in Ref. 103. σ is the localization precision, and ω is the Gaussian standard deviation of a short-range correction term centered at d_c. a, A_1, and A_2 are adjustable parameters.

$$p(d) = A_1\left(\frac{d}{\sqrt{2\sigma^2}}e^{\frac{-a^2}{4\sigma^2}}\right) + A_2\left(\frac{1}{\sqrt{2\pi\omega^2}}e^{\frac{-(d-d_C)^2}{2\omega^2}}\right) \qquad (2)$$

Supplementary Tables

Supplementary Table 1. RNA half-lives measured by RT-qPCR. Half-lives were determined for *ctrA* and 5S RNA in a Δ*hfq* background, for *tmRNA/ssrA*, *rne*, *ctrA*, and *spmX* during exponential, early stationary, and late stationary phases in a wild-type background.

ctrA (Δ*hfq*)	Exponential Phase	0.8 ± 0.1 min
	Stationary Phase	3466 ± 10 min
5S (Δ*hfq*)	Exponential Phase	24 ± 10 min
	Stationary Phase	39 ± 10 min
tmRNA/*ssRA*	Exponential Phase	13 ± 7 min
	Late Stationary Phase	45 ± 12 min
rne (WT)	Exponential Phase	0.48 ± 0.08 min
	Early Stationary Phase	1.2 ± 0.4 min
	Late Stationary Phase	9 ± 4 min
ctrA (wt)	Exponential Phase	0.51 ± 0.06 min
	Early Stationary Phase	0.9 ± 0.2 min
	Late Stationary Phase	102 ± 20 min
spmX (wt)	Exponential Phase	0.5 ± 0.1 min
	Early Stationary Phase	0.81 ± 0.04 min
	Late Stationary Phase	33 ± 17 min

Supplementary Table 2. Strains used in this work

STRAIN	SOURCE	IDENTIFIER
***Caulobacter crescentus* NA1000**	Lucy Shapiro, Stanford University School of Medicine	N/A
NA1000 *rne::rneΔCTD specR*	This paper	*JS769*
NA1000 *spmX::spmX-mEos3.2 specR*	This paper	*JS770*
NA1000 *acnA::acnA-PAmChy specR*	This paper	*JS771*
NA1000 *acnA::acnA-PAmChy rne::rne-eYFP specR gentR*	This paper	*JS772*
NA1000 *rhlB::rhlB-PAmChy SpecR*	This paper	*JS773*
NA1000 *rhlB::rhlB-PAmChy rne::rne-eYFP specR gentR*	This paper	*JS774*
NA1000 *rne::rne-eYFP gentR*	This paper	*JS401*
NA1000 *rne::rne-msfGFP gentR*	Ref. [1]	*JS87*
NA1000 *vanA::Ms2-DM-mChy rne::rne-msfGFP specR/gentR*	Ref. [2]	*JS285*
NA1000 *spmX::ms2 96 array vanA::Ms2-DM-mChy rne::rne-msfGFP specR/kanR/gentR*	Ref. [2]	*JS283*
NA1000 *rsaA::ms2 96 array vanA::Ms2-DM-mChy rne::rne-msfGFP specR/kanR/gentR*	Ref. [2]	*JS287*
NA1000 *rne::rneΔDBS SpecR*	Ref. [3]	*JS801*

NA1000 *rne::rne-ΔDBS-mEos3.2 SpecR*	This paper	*JS804*
NA1000 *hfq::tet rne::rne-mEos3.2C-1 specR/tetR*	This paper	*JS805*
NA1000 *rne::rneΔCTD Kan^R*	This paper	*JS806*
NA1000 *rne::rneΔCTD spmX::spmX-mEos3.2 specR Kan^R*	This paper	*JS807*
NA1000 *hfq::tet tetR*	Ref. [4]	*CJW5477*
NA1000 *hfq::spec SpecR*	Gift of Lucy Shapiro	*JS263*
NA1000 *rne::rne-mEos3.2C-1 SpecR*	This paper	*JS775*
NA1000 *rne::rne-ΔCTD-mEos3.2 SpecR*	This paper	*JS776*
NA1000 *ctrA::ms2 48 array kanR*	This paper	*JS777*
NA1000 *spmX::ms2 48 array kanR*	This paper	*JS778*
NA1000 *rsaA::ms2 48 array kanR*	This paper	*JS779*
NA1000 *ctrA::ms2 48 array vanA::Ms2-DM-mChy rne::rne-msfGFP specR/kanR/gentR*	This paper	*JS780*
NA1000 *spmX::ms2 48 array vanA::Ms2-DM-mChy rne::rne-msfGFP specR/kanR/gentR*	This paper	*JS789*
NA1000 rsaA::ms2 48 array vanA::Ms2-DM-mChy rne::rne-msfGFP specR/kanR/gentR	This paper	*JS790*
Agrobacterium tumefaciens C56 *rne::rne-YFP gentR*	Ref. [1]	*JS5*
Sinorhizobium meliloti *rne::rne-YFP gentR*	Ref. [1]	*JS9*
***E. coli* DH10B**	Thermofisher scientific	EC0113
***E. coli* TOP10**	Thermofisher scientific	*C404010*

Supplementary Table 3. Chemicals, peptides, and recombinant proteins used in this work

ITEM	*SOURCE*	*IDENTIFIER*
Gibson Master Mix	New England BioLabs Inc.	E2611S
L-Azidohomoalanine (AHA)	ClickChemistryTools	1066-25
Paraformaldehyde, 96%	ThermoFisher Scientific	A11313.22
Cy5 Alkyne	ClickChemistryTools	TA116-1
Iodoacetamide	Sigma-Aldrich	144-48-9
THPTA	Click Chemistry Tools	1010-100
Copper (II) sulfate pentahydrate	Sigma-Aldrich	7758-99-8
TRizol Reagent	Ambion	15596018
Spectinomycin	Sigma-Aldrich	S6501-25G
Rifampicin	Sigma-Aldrich	R7382-1G
Kanamycin	Sigma-Aldrich	K1377-5G

Chloramphenicol	Sigma-Aldrich	C0378-25G
Nalidixic Acid	Sigma-Aldrich	N8878-5G
Sucrose	Sigma-Aldrich	S5016-25G
Phusion DNA polymerase	Thermo Scientific	F-530L
RNAprotect Bacterial Reagent	QIAGEN	76506
Luna® Universal One-Step RT-qPCR Kit	NEB	E3005L
Qubit RNA HS Assay Kit	Thermo Fischer Scientific	Q32851
Chloroform	Thermofisher scientific	AC423550010
Glycogen, RNA grade	Thermofisher scientific	RO551
Sodium Ascorbate	Thermofisher scientific	134-03-2
2-PROPANOL, ANHYDROUS	Sigma-Aldrich	67-63-0
ETHANOL-D6 (D, 99%), ANHYD.	Sigma-Aldrich	1516-08-1
EDTA (0.5 M), pH 8.0, RNase-free	Sigma-Aldrich	AM9261
Tris (1 M), pH 7.0, RNase-free	Thermofisher scientific	AM9851
Agar	Thermofisher scientific	DF0001-17-0
Bactopeptone	Fisherchemicals	211677
Yeast extract	Thermofisher scientific	92144-500G-F
UltraPure™ Ethidium Bromide, 10 mg/mL	Sigma-Aldrich	15585011
Thermo Scientific™ TriTrack DNA Loading Dye (6X)	Thermofisher scientific	FERR1161
Magnesium sulfate	Thermofisher scientific	M7506-1KG
Calcium chloride (97%)	Sigma-Aldrich	746495-500G
Potassium phosphate dibasic anhydrous	Sigma-Aldrich	P288-500
Ammonium Chloride (99.5%)	Fisherchemicals	A9434-1KG
Sodium phosphate dibasic	Sigma-Aldrich	S7907-1KG
Luria Broth Base	Sigma-Aldrich	12795084
Iron (II) sulfate heptahydrate	Thermofisher scientific	F8633-250G
FD Dpn1	Sigma-Aldrich	ER1701
T4 DNA Ligase	Thermofisher scientific	EL0011
Agarose	Thermofisher scientific	A7705
RNAprotect Bacteria Reagent	Qiagen	76506
Gentamycin Sulfate	Sigma-Aldrich	345814-1GM
Carbonyl Cyanide *m*-Chlorophenylhydrazone	Sigma-Aldrich	555-60-2
Glucose (99.5%)	Sigma-Aldrich	G8270-1KG
FD EcoR1	Thermofisher scientific	FD0274
FD Nde1	Thermofisher scientific	FD0585
FD Kpn1	Thermofisher scientific	FD0524
Paraffin wax	Sigma-Aldrich	327204-1KG
Oxytetracycline, 96%	Thermofisher scientific	J62427-09
T4 Polynucleotide Kinase (T4 PNK)	New England Biolabs	M0201S

Supplementary Table 4. Primers used for strain construction

ITEM	SEQUENCE
Primer Ups F for JS769 rne::rneΔCTD specR	atctggatccagcgcctgaagagcgtcg
Primer Ups R for JS769 rne::rneΔCTD specR	gttgtcattcttagtcatcgaccacgaccg
Primer Down F for JS769 rne::rneΔCTD specR	cgatgactaagaatgacaacggcccgcg
Primer Down R for JS769 rne::rneΔCTD specR	tagcgaattcgaggaagccctcaagcttg
Primer pNTPS F for JS769 rne::rneΔCTD specR	gggcttcctcgaattcgctagcttcggc
Primer Spec F for JS769 rne::rneΔCTD specR	cgatgactaagatcttttctacggggtc
Primer Spec R for JS769 rne::rneΔCTD specR	gttgtcattcctagatgccgactaccttg
Primer ΔCTD F for JS769 rne::rneΔCTD specR	cggcatctaggaatgacaacggcccgcg
Primer ΔCTD R for JS769 rne::rneΔCTD specR	agaaaagatcttagtcatcgaccacgaccg
Primer pspmX F for JS283 spmX::ms2 96 array vanA::Ms2-DM-mChy rne::rne-msfGFP specR/kanR/gentR	ataaggtacccggcgccggtgctgttcg
Primer pspmX R for JS283 spmX::ms2 96 array vanA::Ms2-DM-mChy rne::rne-msfGFP specR/kanR/gentR	atattagaattcctactcttcgtcgctcacatcggggc
IDT G-block for JS775 rne::rne-mEos3.2C-1 SpecR	ccatggagggcgacaccttctataacaaggtgcgcttctat ggcaccaacttcccggccaatggccccgtgatgcagaag aagaccctgaagtgggaacccagcaccgaaaagatgtac gtgcgcgacggcgtcctgacgggcgacatcgagatggcgc tgctcctggagggcaacgcgcactatcgttgcgatttccgc accacctacaaggcgaaggagaagggcgtgaagctcccg ggcgcccatttcgtcgaccattgcatcgaaatcctgtccca cgataaggattataataaggtgaagctgtacgagcacgcc gtggcgcattccgggctgccggataacgcccgccgttaag ctagcaaagaattcgaacgttacgcgtcaccggtcggcca ccatgtcggcgatcaagccggacatgaagatcaagctgcg catggagggcaatgtgaacgggcaccacttcgtgatcgac ggcgacggcaccgggaagccgttcgagggcaagcagtcg atggacctggaggtcaaggagggcgggccgctccccttcg cgttcgacatcctcacgaccgccttccactacggcaaccg ggtgtttgccaagtatccggacaacatccaggactatttca agcagtcgttcccgaagggctatagctgggagcgctcgctg accttcgaggacggcggtatctgcaacgcccgcaacgac atcaccatggagggcgacaccttctataacaaggtgcgctt ctatggcaccaacttcccggccaatggccccgtgatgcag aagaagaccctgaagtgggaacccagcaccgaaaagat gtacgtgcgcgacggcgtcctgacgggcgacatcgagatg gcgctgctcctggagggcaacgcgcactatcgttgcgattt ccgcaccacctacaaggcgaaggagaagggcgtgaagct

	cccgggcgcccatttcgtcgaccattgcatcgaaatcctgt cccacgataaggattataataaggtgaagctgtacgagca cgccgtggcgcattccgggctgccggataacgcccgccgt taagctagcaaa
Primer HY118F for JS776 rne::rne-ΔCTD-mEos3.2 SpecR	attgcatatgccacgcgcgagcgcaaca
Primer HY118R for JS776 rne::rne-ΔCTD-mEos3.2 SpecR	cgttcgaattgtcatcgaccacgaccgacacg
Primer HY117F for JS776 rne::rne-ΔCTD-mEos3.2	ggtcgatgacaattcgaacgttacgcgtc
Primer HY115R for JS776 rne::rne-ΔCTD-mEos3.2	tcgcgcgtggcatatgcaattggacgtctc
Primer HY116F for JS770 spmX::spmX-mEos3.2 specR	attgcatatgacaagcttctgaacaggc
Primer HY116R for JS770 spmX::spmX-mEos3.2 specR	cgttcgaattctcttcgtcgctcacatc
Primer HY115F for JS770 spmX::spmX-mEos3.2 specR	cgacgaagagaattcgaacgttacgcgtc
Primer HY115R for JS770 spmX::spmX-mEos3.2 specR	agaagcttgtcatatgcaattggacgtctc
Primer HY120F for JS804 rne::rne-ΔDBS-mEos3.2 SpecR	attgcatatgagcctgcacgcgggcgac
Primer HY120R for JS804 rne::rne-ΔDBS-mEos3.2 SpecR	cgttcgaattcggcgcggtgatctcgttcg
Primer HY119F for JS804 rne::rne-ΔDBS-mEos3.2 SpecR	caccgcgccgaattcgaacgttacgcgtc
Primer HY119R for JS804 rne::rne-ΔDBS-mEos3.2 SpecR	cgtgcaggctcatatgcaattggacgtctc
Primer HY1'F for JS806 NA1000 rne::rneΔCTD KanR	ggtcgatgactaagctagctgcagcccg
Primer HY1'R for JS806 NA1000 rne::rneΔCTD KanR	agctagcttagtcatcgaccacgaccgac
Primer HY24F for JS771 acnA::acnA-PAmChy specR	ggtcggccacatggtgagcaagggcgag
Primer HY24R for JS771 acnA::acnA-PAmChy specR	ctgcagctagttacttgtacagctcgtccatg
Primer HY23F for JS771 acnA::acnA-PAmChy specR	gtacaagtaactagctgcagcccggggg
Primer HY23R for JS771 acnA::acnA-PAmChy specR	tgctcaccatgtggccgaccggtgacgc
Primer HY47F for JS771 acnA::acnA-PAmChy	ccttaattaacaaccgcatcaccccgga
Primer HY47R for JS771 acnA::acnA-PAmChy	cgaattctccgtcggccttggccaggtt
Primer HY48F for JS771 acnA::acnA-PAmChy	caaggccgacggagaattcgaacgttacg
Primer HY48R for JS771 acnA::acnA-PAmChy	gatgcggttgttaattaaggcgcctgcag

Primer HY49F for JS773 rhlB::rhlB-PAmChy SpecR	ccttaattaacgcaccatgccgacgactatgtccaccg
Primer HY49R for JS773 rhlB::rhlB-PAmChy SpecR	cgaattctcccttcgcgccgcgcggcgg
Primer HY50F for JS773 rhlB::rhlB-PAmChy SpecR	cggcgcgaagggagaattcgaacgttacg
Primer HY50R for JS773 rhlB::rhlB-PAmChy SpecR	gcatggtgcgttaattaaggcgcctgcag
IDT G-block for JS777 ctrA::ms2 48 array kanR	caattggatccaatcttgacgtccgtttgattacgatcaaga ttggatccaataggtcgccgaaccacgatgcgaggaaacg catatgtcgaagaagcctgcaggcgccttaattaatatgca tggtaccttaagatctcgagctccggagaattcgaacgtta cgcgtcaccggtcggccaccatggtgagcaagggcgagg agctgttcaccggggtggtgcccatcctggtcgagctggac ggcgacgtaaacggccacaagttcagcgtgtccggcgagg gcgagggcgatgccacctacggcaagctgaccctgaagtt catctgcaccaccggcaagctgcccgtgccctggcccac cctcgtgaccaccctgacctggggcgtgcagtgcttcagc cgctaccccgaccacatgaagcagcacgacttcttcaagt ccgccatgcccgaaggctacgtccaggagcgcaccatctt cttcaaggacgacggcaactacaagacccgcgccgaggt gaagttcgagggcgacaccctggtgaaccgcatcgagctg aagggcatcgacttcaaggaggacggcaacatcctgggg cacaagctggagtacaactacatcagccacaacgtctata tcaccgccgacaagcagaagaacggcatcaaggccaac ttcaagatccgccacaacatcgaggacggcagcgtgcag ctcgccgaccactaccagcagaacaccccatcggcga cggccccgtgctgctgcccgacaaccactacctgagcac ccagtccgccctgagcaaagaccccaacgagaagcgcg atcacatggtcctgctggagttcgtgaccgccgccgggatc actctcggcatggacgagctgtacaagtaatctagaagctc ggtattcctgagcttgttaacaccgatccgcatggcaccgtt tcggtgtgcgtaggagggtgattgcgcggtagtcctgcgcat agtggaaataccttagccagccctttaaaatgcggtatgtc acaaggtacagggcgtattcgtccctgtacgaagagcacc tttcggtagcgtctaactacacctcctgtcctcgaatcgcag ggtattcctctgcgtaggtgtcggagtgtgacgcatagttcca accgtcacagggacccttgataatggggtattcctccattg acacacgatacgcttcacgtaaatatacggacagtccgtt cttcataacagaagcgtaatcgtcttctctcttctttgccagc cgcggtcatcgccatgcaagaaatatcgcagcacttggtc ggtagtcctgaccacaaggctgacgcctagtctttacagct gcctactgcccttatcggtgcaacatgcggtaatcctgcat gctaacttgttcatactatataggatgtgtttgctgccgcaga aataaacccacgcggtaatcctgcgtgcgttctagtgtcttg cgtgagcggtagcctggcatcagccatgccccggatgtgg ggtagtcctccacaaagggagaacatccatatatagtggg gagtctctcgtataagtgcttatgcacagggtattcctctgtg

tattgagtatgaatcgactccctggaagaaagagtatatttc
tccttgccgacgcggtagtcctgcgtcattgccgccaggtg
gcgacgctcggttgatgcctgaaagcatttcaccgaagctc
ggtattcctgagctaagcttgaactgttccccaagggtcggt
ctacaggctgtggcgtcacacatgcgcggtagtcctgcgca
ccagcttggatgtcctcgcgactctttagatgtcttggagca
ggagcaggcagggcgtattcgtccctgcgagaatagtgctt
gaggttcgaaacaggacatacatcttgagagaaagccgca
gggtattcctctgcgcggcgagacggcctacgcagactaa
cgtataatacatcaaacatgtcgtgaatggggtattcctcca
ttcctaataggattgtgtaagaaggcgaggtgcagtggctgc
taaactctatagaagcgtaatcgtcttctcaatcgagtataa
ctatttgaatgcgcgctactcgcaggcatagccaatgtggtc
ggtagtcctgaccatggttaaccaggcaccgccctgtcga
atatccgggtcacaataggctttgcatgcggtaatcctgcat
gtaatagctcgtatgtggtgtccggtcccggttaacaagctt
atgacgtaccacgcggtaatcctgcgtgatctgaatgtgaa
tcgcgtagcatgtgcggggtgcaacgttcgagttcggtgtgg
ggtagtcctccacaacttcaccgctagatcaccattggtct
cagagccataatagtcctgctaacacagggtattcctctgt
ggccatagggtcatgtgcgtgatccgcgtcgtccgggtatag
agttaatgagacgcggtagtcctgcgtccccgcatgcatgt
gccggaatgctccgctacccactcggtttataaattgagct
cggtattcctgagctgatctaagagaaacagcgcgatcatc
tgacaccaacttgatactgatcgctgcgcggtagtcctgcg
cacggctccaatcacaccagccatgtagtgagtatactcc
tcatgcgtatcccagggcgtattcgtccctgactctgcgtac
atcggatccccgctccgaccacactccagaccacggagc
cgcagggtattcctctgcgaatggggtattcctccattgtgc
gaaaaactgcgtggtagacatcctgacgaaattcagggca
atagcgagaagcgtaatcgtcttcttcgttgggcgcgcccg
cgaccagatgctatgcaacttgcagctgagaatctggtcgg
tagtcctgaccagggtcgtcagctgatcgacaagctggttg
gcagtgttatcgatgtgcatgcatgcggtaatcctgcatgtg
cctgcctttaatggtgcgattgtgttgttccgccatgagatgg
gagtacacgcggtaatcctgcgtgcacttgccgacattcta
gtctctataaggcaactgtgtccagaggcgttatgtggggta
gtcctccacacgttagatagttctaggctcagtttgagggat
ctcacatgtctagctccccacagggtattcctctgtggtgga
taattcgctactctcactgcttctgtaaacgaaaagagatag
aatgacgcggtagtcctgcgtcatggaggaggttatcgtag
cgtattcatcttatctacaatcaagaacgcgagctcggtatt
cctgagctcagcgggctctgatagaattgcatgtctttgggc
actgttaagatatcgttgcgcggtagtcctgcgcacacatga
tagtgcctctggatccttaggtctcgaccaccatgtgactaa
ccagggcgtattcgtccctgctcattgttctcggtggacgttg
gttgaaacagggctttgtagagtcatccgcagggtattcctc
tgcgttccctccagggacattatcgggaccattagtatggcg

	caaattctgataaatggggtattcctccatttagtcctacga cacttccgatgtacagaagggccaccacattcatagacga gaagcgtaatcgtcttctcacgccaggttcccccaagttag gggactgcgcgggtggcccccccccgctggtcggtagtcc tgaccaagtacaacccactaaccagaacaccgctccctg gggatctttgcaatgatcatgcggtaatcctgcatgcgcata agggaaacacgcaaaaccacgaggtcgacgggagccgc aacacgcacgcggtaatcctgcgtgtcacaccaaccata gggaaacgacgcgactggttgcttcgacagcctgcgtgtgg ggtagtcctccacagagatccggcgcgagacatggtgcac catgcagaggcgtagagagctccgcacagggtattcctctg tgacaaactaacaggttatctaggaagattcggccaaccgt cggtaatactagacgcggtagtcctgcgtcgctagcataaa acgaaaggctcagtcgaaagactgggcctttcgttttatctg ttgtttgtcggtgaacgctctcctgagtaggacaaatccgcc gggagcggatttgaacgttgcgaagcaacggcccggaggg tggcgggcaggacgcccgccataaactgccaggcatcaa attaagcagaaggccatcctgacggatggcctttcgatcg
Primer HY55F for JS777 ctrA::ms2 48 array kanR	gccaccatggtctagaagctcggtattcc
Primer HY55R for JS777 ctrA::ms2 48 array kanR	gaacctcaagcactattctcgcagggac
Primer HY53F for JS777 ctrA::ms2 48 array kanR	ctttcgatcggctagctgcagcccgggg
Primer HY53R for JS777 ctrA::ms2 48 array kanR	agcttctagaccatggtggccgaccggtg
Primer HY63F for JS777 ctrA::ms2 48 array kanR	gcatggtacctcgtcggaaatcgacacc
Primer HY63R for JS777 ctrA::ms2 48 array kanR	ttcgaattcttcaggcggcgttaacctg
Primer HY64F for JS777 ctrA::ms2 48 array kanR	cgccgcctgaagaattcgaacgttacgc
Primer HY64R for JS777 ctrA::ms2 48 array kanR	tttccgacgaggtaccatgcatattaattaag
Primer HY57F for JS778 spmX::ms2 48 array kanR	gcatggtaccacaagcttctgaacaggc
Primer HY57R for JS778 spmX::ms2 48 array kanR	ttcgaattctctactcttcgtcgctcac
Primer HY58F for JS778 spmX::ms2 48 array kanR	cgaagagtagagaattcgaacgttacgc
Primer HY58R for JS778 spmX::ms2 48 array kanR	agaagcttgtggtaccatgcatattaattaag
Primer HY61F for JS779 spmX::ms2 48 array kanR	gcatggtacctcgacgccagcgccgtca
Primer HY61F for JS779 spmX::ms2 48 array kanR	ttcgaattctttaggcgagcgtcaggacttcg

Primer HY62F for JS779 spmX::ms2 48 array kanR	gctcgcctaaagaattcgaacgttacgc
Primer HY62F for JS779 spmX::ms2 48 array kanR	ctggcgtcgaggtaccatgcatattaattaag

Supplementary Table 5. mRNA FISH probes used in this work.

ctrA probes	*spmX* probes	*rsaA* probes
taatggtgaatgtttcccgt	agtttgagacagacgcggat	gtgtacgcagtcaccaactg
cactttgccggagagttaat	gtttcatcgcctagattgac	tctgggtttgagtcgcgtac
tggcgtattcgaacgtcttt	tcttgatgagatcgacggcg	taggtctggatggcaacagc
catcctcgatcaacagtacg	ttctgacggtacccttcgaa	ggcaacgccggtgaagaact
ttcagacttcagcatcagtt	cgtccttttccgagacagag	tggtcgagtcgaccaggaag
tccgtcgtatagacgttgaa	tgagatcatagagcagcagc	aacttcgagtagtacgcgtc
tagatcttgcccagatcgac	gtgtgctcgttcaccgaatg	gatgaagcggttttcctgag
gagcaggataagatcgtagt	tcgaactggttctggttcag	tggccaggttgatcgagaag
tcatgtccggaagattgagg	tattgaaggcgaagcacacc	cgtacgaaacgcccgtgtag
agggtgcgcagaacatcgat	gagcggaggaagttgtcgag	cgatgatcttgtcataggcg
atcatgatgggcgtgttgat	aaccagtgcatcgatgacga	cggtcaggtagtcgatgttg
ttgaccttggtgtcgatttc	cgtgaggaacagagtcttct	ttgacggccagatcgatgtc
cttggtcatgtagtcgtcgg	tcatagtcgaccttgggacg	ttcaggatggtgccgatcag
atcatttcgtccttgtggaa	cggaacggcgtgaactcgac	cgacaggtcgttgatcatcg
tgacccttcgaacgacggac	ctgttcagaagcttgtggcg	gacggataggcggtgaacag
cggtcttgatgaccgactgg	gattaaagaccgacgagccg	tggtcagcgagagggtcgaa
acaggtggttcaggaacatt	tgatcagcaggctggtgttg	aacgaacgtgtcgttgttgg
gtcgatgatcttcagttccg	acggtcaggatccagaggac	tcacgttcatcgtttcgatg
tgcgcagcttgcagatgaag	tagccgaagagcttgacctg	aagacgtgttcagggtgatc
cagaccgtctcaatgtggtg	cgagaccacgaagcagatcg	ttgcgtcaacgtggtgttca
aacgactcaggcggcgttaa	cgaggcaagaaacctactct	agagtcggtgatcgtcacag
tgggttctacagatacgctg		caggttgacggtcgtcagag
agaaaacgcccacctttgg		gtcagaccattgacgttcag
		ggtgaaaccatcgtcagcag
		tcgaaccagcgatgttgatg
		cgagatgttcagggtcgtcg
		tgtgcgaggtgatcgtgacg
		ttgacgttggccaccagaac
		gtcagcgctgaacgacgaac
		cgacgcggagggtttcgaag
		caacgttggtgaaggtcgtc
		agaacggtcaggccgacatt

		gacagggtcaggttgaacac
		cgtcaccacgatcgacttgg
		ggtgttggtcaggttcagac
		acacgaaggtcacagccgag
		gcggatcgtgacgacttcac
		caccgatgatggtgtcattg
		gatatcgaagatatccgcgc
		gtcggtgatcgtcacgaaag
		ttcgtcgagatgccgacgag
		aactggaaccacttggcaac
		gtcaacgacgacataggtgt
		agaccggtcagcttgatcac
		tcaggacttcggtggcgaag

Supplementary References

1. Al-Husini, N., Tomares, D. T., Bitar, O., Childers, W. S. & Schrader, J. M. α-Proteobacterial RNA Degradosomes Assemble Liquid-Liquid Phase-Separated RNP Bodies. *Mol. Cell* **71,** 1027-1039.e14 (2018).
2. Al-Husini, N., Tomares, D. T., Pfaffenberger, Z. J., Muthunayake, N. S., Samad, M. A., Zuo, T., Bitar, O., Aretakis, J. R., Bharmal, M.-H. M., Gega, A., Biteen, J. S., Childers, W. S. & Schrader, J. M. BR-Bodies Provide Selectively Permeable Condensates that Stimulate mRNA Decay and Prevent Release of Decay Intermediates. *Mol. Cell* **78,** 670-682.e8 (2020).
3. Passos, C., Tomares, D., Yassine, H., Schnorr, W., Hunter, H., Wolfe-Feichter, H. K., Velier, J., Dzurik, K. G., Grillo, J., Gega, A., Saxena, S., Schrader, J. & Childers, W. S. BR-Bodies Facilitate Adaptive Responses and Survival During Copper Stress in Caulobacter crescentus. 2025.03.11.642215 Preprint at https://doi.org/10.1101/2025.03.11.642215 (2025)
4. Irnov, I., Wang, Z., Jannetty, N. D., Bustamante, J. A., Rhee, K. Y. & Jacobs-Wagner, C. Crosstalk between the tricarboxylic acid cycle and peptidoglycan synthesis in Caulobacter crescentus through the homeostatic control of α-ketoglutarate. *PLOS Genet.* **13,** e1006978 (2017).